Materials Research Proceedings 39 (2024) 42-50 https://doi.org/10.21741/9781644903094-6

Numerical Investigation on Deformation Behavior of Aluminium Foams with *in situ* Composite Particles

M. Rakesh[1,a], A. Tewari[1] and S. Karagadde[1,b]

[1]Department of Mechanical Engineering, Indian Institute of Technology Bombay, Mumbai, India

[a]merugurakesh94@gmail.com, [b]s.karagadde@iitb.ac.in

Keywords: Metal Matrix Composite, *in situ* Metal Foam, Finite Element Analysis, Liquid Metallurgy Process, Energy Absorption

Abstract. Metal foams are cellular solids with high stiffness, high strength and superior energy absorption capacity. In liquid metallurgy, foams are processed by foaming the molten metal with the addition of foaming agents and stabilized by the presence of particles which also strengthen the cell walls. An analysis of the deformation behaviour of foams in the presence of these stabilizing particles is essential to the mechanism of energy absorption. In the present study, the effect of the particle distribution on the deformation behaviour of the closed-cell aluminium foams was investigated using Finite Element Analysis (FEA) in Abaqus© software. The experimental data were used to model the distribution of particles in the matrix and the foam model. The simulation results were validated with the experimental results. The uniform distribution of particles in the matrix resulted in lower stress concentration and enhanced the mechanical performance of composite material and the metal foam.

Introduction

Metal foams are lightweight materials with high stiffness, high specific strength-to-weight ratio and superior specific energy absorption capacity [1–3]. Processing of metal foams through the liquid metallurgy route involves, melting and foaming of molten metal or alloy by the addition of foaming agents such as TiH_2 or $CaCO_3$ in the presence of stabilizing particles to obtain a uniform foam structure. The properties of foam mainly depend on the structure of the foam, distribution of pore size and cell wall thickness, and the type of particles used and their distribution for stabilization [4, 5]. The particles used for the foam stabilization were added externally (*ex situ*) or generated internally using *in situ* chemical reaction with the matrix material. It is well known that *in situ* particles exhibit superior bonding strength, wetting behaviour and nucleation potency with the primary phase over the *ex situ* particles and efficiently stabilise the foam structure [6–8]. Nevertheless, the particles tend to form clusters near the cell walls and plateau borders when the metal foams are processed through the liquid metallurgy route. Studying the role of these particle clusters on the properties of foam is necessary to understand the deformation behaviour of foam.

FEA is a numerical technique widely used to analyse the elastic-plastic behaviour of heterogeneous materials such as Metal Matrix Composites (MMC) and metal foams [9]. Ma *et al* numerically investigated the mechanical and fracture behaviour of particle reinforce A356 composite with 2D representative volume element (RVE) models and reported that, the simulation results closely matched the experimental results with the use of damage evolution criteria [10, 11]. Antunes *et al* developed a new model for estimating the flexural properties of epoxy and polyester resin-based syntactic foams and concluded that the flexural stiffness decreased with the filler volume fraction and epoxy-based foams outperformed polyester foams [12]. Nammi *et al* analysed the quasi-static loading of closed-cell aluminium foams using the repeating unit cell method based on the tetrakaidekahedral model and accurately estimated the crushing resistance of the foam [13]. Perez *et al* estimated the properties of CNT-reinforced aluminium metallic foams and found that Young's modulus prediction using FEA analysis was within the theoretical values and smaller

pores lead to lower values of elastic modulus [14]. Karan *et al* predicted the compressive deformation behaviour of LM 13 aluminium foam in accordance with the experimental results. However, the role of particle distribution on the properties of metal foams has not been studied in detail in the past which is essential to understand the deformation of behaviour of metal foam during mechanical testing in turn to optimise the process parameters.

In the present study, the effect of particle clusters on the deformation behaviour of metal foams was investigated using 2D FEM (Finite Element Method). 2D FEM was widely used to study the stress and strain distributions for multi-scale simulations, especially for MMCs [15], but it was limited to planar deformations with a strong dependency on the domain size. However, it will provide insights into the initial approximations of stress-strain behaviour of multi-scale models. Among various types of *in situ* particles that were analysed in the previous studies, *in situ* Al_3Zr particles that possess low density (4.11 g/cm^3), high stiffness (150 GPa) and high melting point (1580 ºC), have shown better stabilisation of the foam with uniform pore distribution and good nucleation potency with the primary phase [16–18] and are employed in the present investigation. 2D RVE models were used to analyse the fracture behaviour of MMC with *in situ* Al_3Zr particles. The constitutive behaviour of MMCs was used to perform the deformation simulations of foam structures.

Numerical methodology

The numerical investigation was carried out in two stages. Initially, the properties of MMC with uniform and clustered distributions of particles were analysed. In the later stage, the constitute behaviour of MMCs obtained from the simulation was used to study the deformation behaviour of metal foams with compression simulation.

a). Simulation of MMC

Different sizes of 2D RVE models were employed to analyse the deformation and damage behaviour of A356 with *in situ* Al_3Zr particles. The 2D RVE models were generated using in-house Python code that was implemented using Abaqus© software. The particle generation takes place if the particle was not overlapping with the previously existing particle and in contact with the edges of the RVE. This operation was repeated till the desired volume fraction of the particle was obtained. The particle distribution varied by varying the coefficient of variation of the nearest neighbour distance (COV_d) of the particle which is the ratio of the standard deviation of the particle size distribution to the mean nearest neighbour distance of the particle [19].

The MMC samples were prepared for metallography to measure the size distribution of Al_3Zr particles in the matrix. From the metallography of the Al_3Zr particles, the shape of the particle was identified as a rectangle of length 11.2± 0.62 μm and width of 7.3±0.61 μm. For modelling cluster distribution, a COV_d value of 0.325 was used, while for uniform distribution a value of 0.062 was employed. The properties of A356 alloy are adopted from the literature [20]. The properties of particles are calculated from the reverse solution algorithm proposed by Dao *et al* [21]. The input parameters (Nano-indentation results) required for the algorithm are shown in Table 1, where υ is Poisson's ratio, C is the loading curvature, h_r/h_m is the ratio of residual indentation depth to maximum indentation depth, P_{ave} is the average load and P_m is the maximum load. The parameters calculated from the reverse solution algorithms are shown in Table 2. Where $\sigma_{0.033}$ is actual stress at 0.033 strain, E is Young's modulus, n is strain hardening exponent and σ_y is yield stress. Fig. 1 shows the stress-strain behaviour of the matrix and particle implemented in the simulation. The periodic boundary conditions and loading on the RVE with uniform and clustered are shown in Fig. 2a and 2b respectively. For modelling the damage evolution in MMC, ductile damage criteria were assigned for matrix material while brittle cracking criteria were assigned for particle material.

Materials Research Proceedings 39 (2024) 42-50 https://doi.org/10.21741/9781644903094-6

The stress-strain behaviour was obtained from the homogenization method proposed by Okereke and Akpoyomare's work [22, 23].

Table 1. Input parameters for the Al_3Zr phase used for the reverse solution algorithm

v	C/GPa	h_r/h_m	P_{ave} (GPa)	P_m (mN)
0.185	198	0.757	7.204	10

Table 2. Parameters obtained for the Al_3Zr phase used for the reverse solution algorithm

$\sigma_{0.033}$ (Mpa)	E (GPa)	n	σ_y (MPa)
1864.77	146.17	0.651	283.5

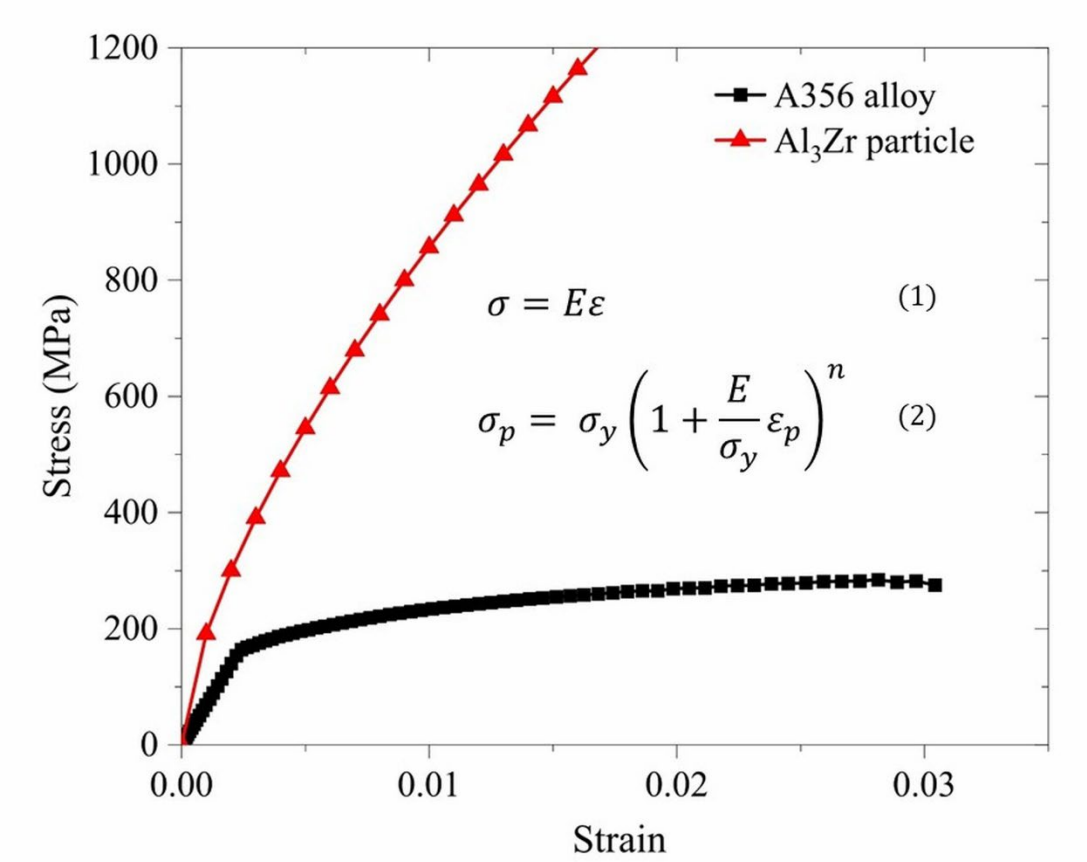

Figure 1. The stress-strain relationship of A356 alloy and Al_3Zr particle calculated from the reverse algorithm

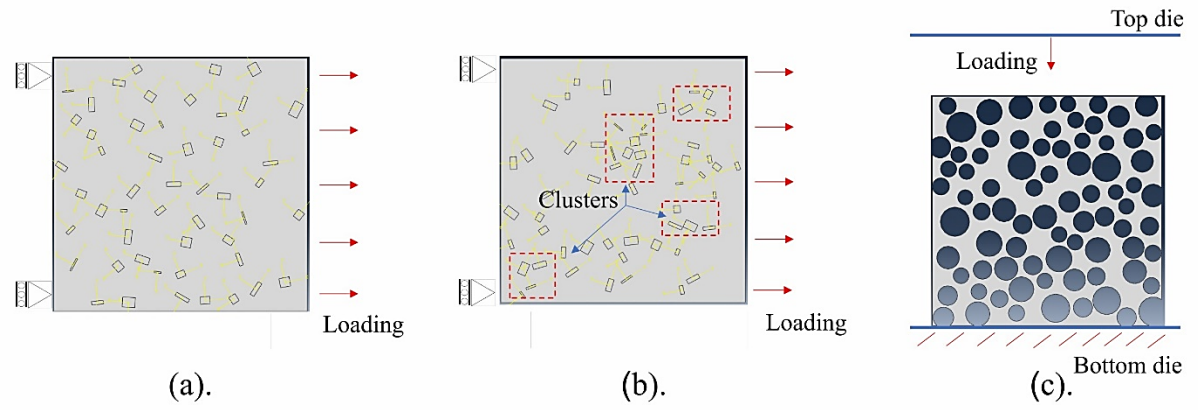

Figure 2. Boundary conditions on (a) uniform distributed RVE, (b) clustered distributed RVE, and (c) foam model

b). Simulation of foam

The structure of foam was generated with a random distribution of pores of 0.8±0.15 mm diameter with 50% porosity. The size of the foam model was a square of length 25mm and meshed with ~ 40000 elements of CPS4R type. The wall thickness (0.08 ±0.012 mm) was varied based on the experimental data. The boundary conditions and the load applied on the foam model are shown in Fig. 2c. Elastic-plastic model was employed for the foam structure in the compression simulation.

Results and discussions

Different sizes of RVE were tested as shown in Fig. 3a and 200 µm with dense mesh (1 µm) with ~ 50,000 elements (CPS4R) was selected to simulate the properties of all microstructural features as well as to minimize the computing time. The effect of particle distribution for 200 µm sized RVE is shown in Fig. 3b, the decrease in stress showed similar behaviour for all the models however the strain values vary because of different particle arrangements, however, the change was minimal. The flow curves of A356/Al_3Zr composite with uniform distribution of particles, from the simulation and experimental are shown in Fig. 3c. The simulation results at 5 wt.% Al_3Zr showed similar deformation behaviour as of experimental results. The results were slightly overestimated as a consequence of the work hardening model included in the simulation model, which is similar to the work done by Zhou *et al* [24]. The overestimation of the flow curve may also be due to the presence of clusters in the experimental samples, which can hinder the strength of the composite. For the cluster distribution of particles, the stress drop occurred at a low value of strain when compared with the uniform distribution. At higher particle concentrations the distance between the neighbouring particles decreases as a result the change in the failure strain for the cluster and uniform distributed case are similar.

Materials Research Proceedings 39 (2024) 42-50 https://doi.org/10.21741/9781644903094-6

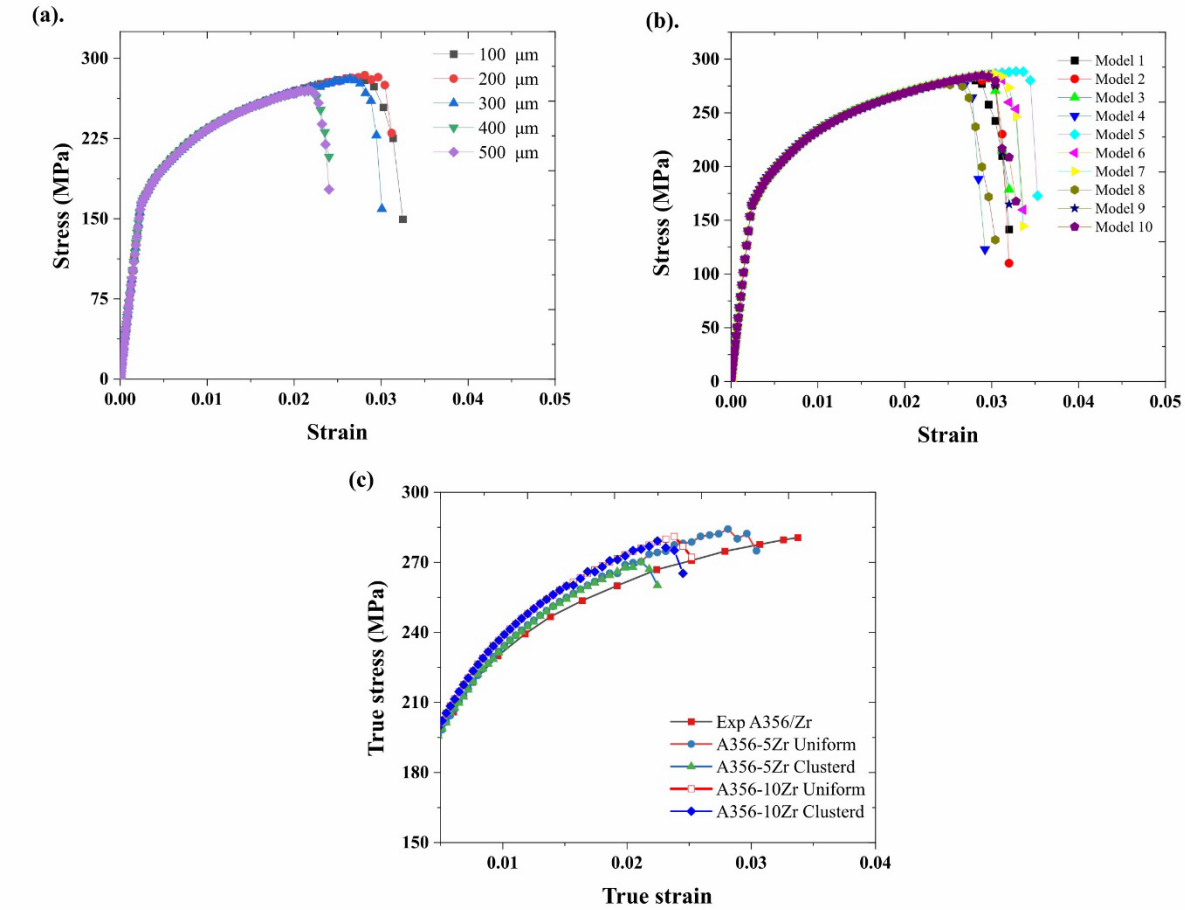

Figure 3. Simulated stress-strain behaviour of A356/Al_3Zr alloy with a). five RVE sizes, b). ten models of 200 µm RVE size, and c) different particle volume fractions and comparison with experimental results.

The Von Mises stress distribution and damage evolution of RVE models with uniform and cluster distribution of *in situ* particles was presented in Fig. 4a and 4b corresponding to the flow curves in Fig. 3c. For the composite with uniform particle distribution the crack initiated within the particle and at the interface with the matrix and propagated at an angle of 45° into the matrix, representing a shear type of fracture (ductile damage) in the matrix. For clustered particle distribution, the cluster served as a stress concentration and both brittle and ductile type of damage evolution is observed. The fracture of the composite occurred at lower strains compared with uniform distribution because of higher stress concentrations and lower tortuosity for crack propagation.

Materials Research Proceedings 39 (2024) 42-50 https://doi.org/10.21741/9781644903094-6

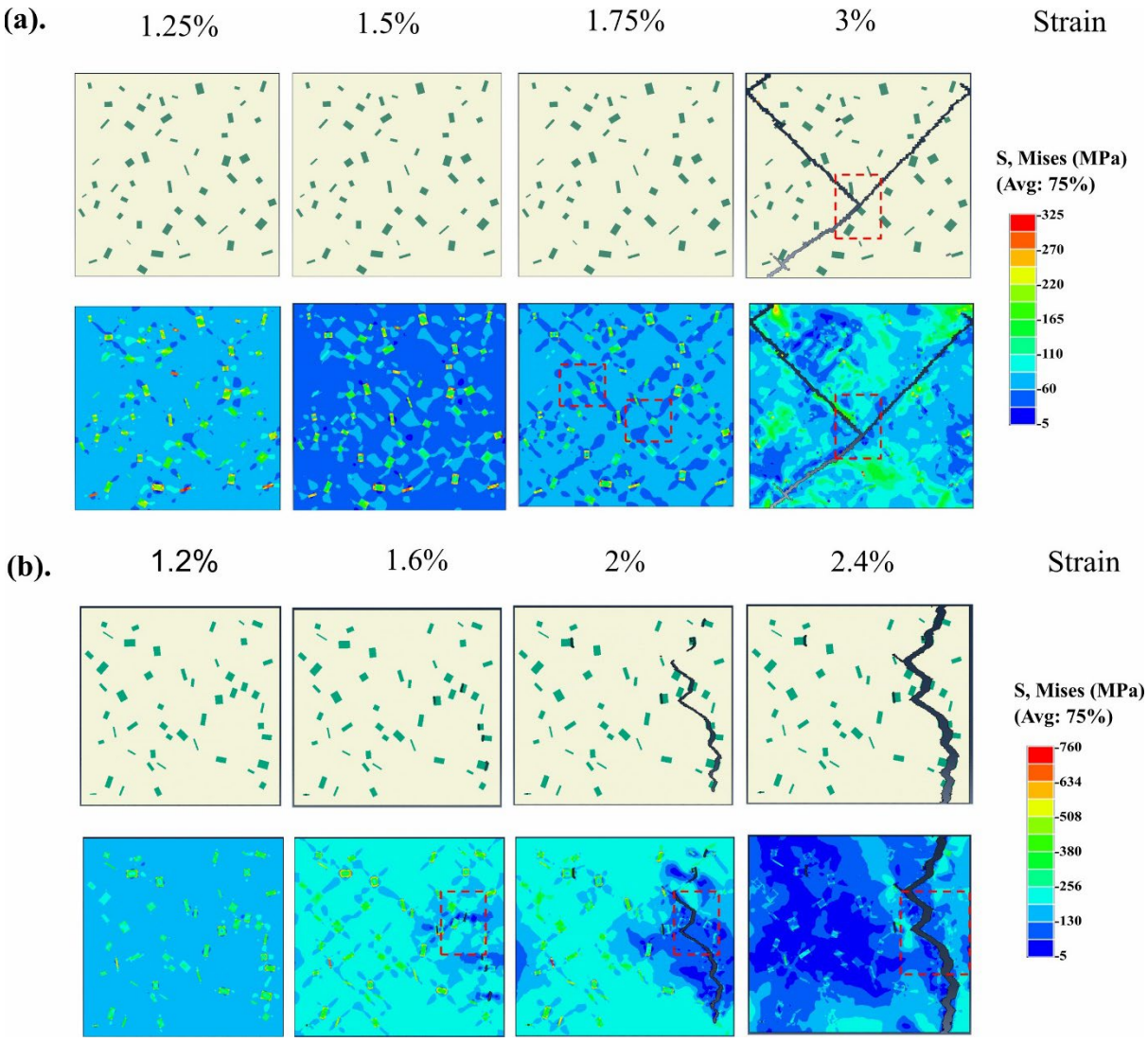

Figure 4. Von Mises stress distribution and damage evolution in A356/Al_3Zr RVE models during tensile deformation in the horizontal direction with a) uniform particle distribution, and (b) clustered particle distribution

The deformation behaviour of A356/Al_3Zr composite metal foam is shown in Fig. 5a, elastic, plateau and densification regions were observed in the simulated results. The deformation bands were formed at 20% strain followed by collapse of the cell wall and densification. The stress-strain behaviour of the composite foam was presented in Fig. 5b. The foam model was validated with pure Al foam and A356/Al_3Zr composite foam with similar properties adopted from previous experimental studies [25, 26]. The experimental and simulation results exhibited similar stress-strain behaviour.

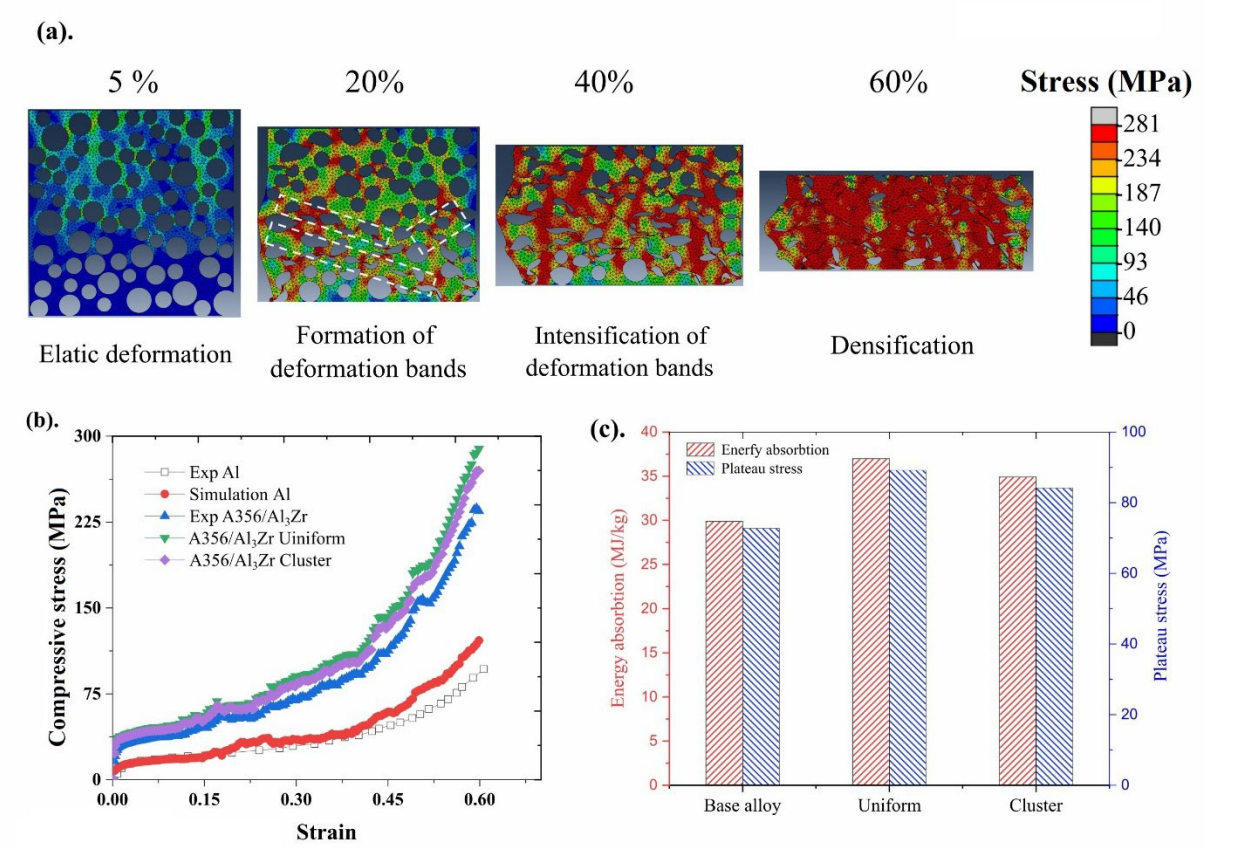

Figure 5. (a). Von Mises stress distribution and deformation behaviour of A356/Al_3Zr foam, and b). compresive stress-strain curves of simulated results and comparison with the experimental data, (c). comparison of plateau stress and energy absorption capacity of foam with uniform and clustered distribution of particles.

The mechanical properties of the composite metal foams were calculated from the simulated stress-strain curves according to ISO 13314 standard [27]. The plateau stress and the energy absorption capacity of the composite foam with the uniform and clustered particle distribution enhanced by 24% and 17% when compared with the base alloy as presented in Fig. 5c. Hence, the composite foam shows better properties when the particles are distributed uniformly within the matrix. The effect of particle shape and size and pore distribution may be studied in future. with two and three-dimensional models of foam to accurately predict the foam properties and optimize the process parameters.

Conclusions

- Numerical simulation modelling of *in situ* foam with uniform and clustered distribution were performed successfully in this study.
- In MMC, the particle fracture was observed followed by initiation and propagation of crack during plastic deformation.
- The simulation results indicated that *in situ* MMCs exhibited improved properties with the use of uniform distribution of particles, this was attributed to lower stress concentration and delay in crack initiation and propagation. However, the mechanical performance of the composite with a cluster distribution with a COV_d of 0.325, and severe stress concentrations lowered the mechanical performance of the composite.
- Similarly, the uniform foam model exhibited better performance due to the enhanced properties of cell wall material.

References

[1] Gibson, L.J., Ashby, M.F.: Cellular Solids. Cell. Solids. (1997). https://doi.org/10.1017/cbo9781139878326

[2] Banhart, J.: Manufacture, characterisation and application of cellular metals and metal foams. Prog. Mater. Sci. 46, 559–632 (2001). https://doi.org/10.1016/S0079-6425(00)00002-5

[3] Banhart, J.: Aluminium foams for lighter vehicles. Int. J. Veh. Des. 37, 114–125 (2005). https://doi.org/10.1504/IJVD.2005.006640

[4] Banhart, J.: Metal foams: Production and stability. Adv. Eng. Mater. 8, 781–794 (2006). https://doi.org/10.1002/adem.200600071

[5] Simone, A.E., Gibson, L.J.: Aluminum foams produced by liquid-state processes. Acta Mater. 46, 3109–3123 (1998). https://doi.org/10.1016/S1359-6454(98)00017-2

[6] Li, D.W., Li, J., Li, T., Sun, T., Zhang, X.M., Yao, G.C.: Preparation and characterization of aluminum foams with ZrH2 as foaming agent. Trans. Nonferrous Met. Soc. China (English Ed. 21, 346–352 (2011). https://doi.org/10.1016/S1003-6326(11)60720-6

[7] Rakesh, M., Srivastava, N., Bhagavath, S., Karagadde, S.: Role of In Situ Formed (Al3Zr + Al3Ti) Particles on Nucleation of Primary Phase in Al-5 wt.% Cu Alloy. J. Mater. Eng. Perform. 2, (2023). https://doi.org/10.1007/s11665-023-08417-z

[8] Atturan, U.A., Nandam, S.H., Murty, B.S., Sankaran, S.: Processing and characterization of in-situ TiB2 stabilized closed cell aluminium alloy composite foams. Mater. Des. 101, 245–253 (2016). https://doi.org/10.1016/j.matdes.2016.03.153

[9] Chawla, N., Sidhu, R.S., Ganesh, V. V.: Three-dimensional visualization and microstructure-based modeling of deformation in particle-reinforced composites. Acta Mater. 54, 1541–1548 (2006). https://doi.org/10.1016/j.actamat.2005.11.027

[10] Ma, S., Wang, X.: Mechanical properties and fracture of in-situ Al3Ti particulate reinforced A356 composites. Mater. Sci. Eng. A. 754, 46–56 (2019). https://doi.org/10.1016/j.msea.2019.03.044

[11] Ma, S., Zhang, X., Chen, T., Wang, X.: Microstructure-based numerical simulation of the mechanical properties and fracture of a Ti-Al3Ti core-shell structured particulate reinforced A356 composite. Mater. Des. 191, 108685 (2020). https://doi.org/10.1016/j.matdes.2020.108685

[12] Antunes, F. V., Ferreira, J.A.M., Capela, C.: Numerical modelling of the Young's modulus of syntactic foams. Finite Elem. Anal. Des. 47, 78–84 (2011). https://doi.org/10.1016/j.finel.2010.09.007

[13] Nammi, S.K., Myler, P., Edwards, G.: Finite element analysis of closed-cell aluminium foam under quasi-static loading. Mater. Des. 31, 712–722 (2010). https://doi.org/10.1016/j.matdes.2009.08.010

[14] Pérez, L., Mercado, R., Alfonso, I.: Young's modulus estimation for CNT reinforced metallic foams obtained using different space holder particles. Compos. Struct. 168, 26–32 (2017). https://doi.org/10.1016/j.compstruct.2017.02.017

[15] Shen, H., Brinson, L.C.: Finite element modeling of porous titanium. Int. J. Solids Struct. 44, 320–335 (2007). https://doi.org/10.1016/j.ijsolstr.2006.04.020

[16] Srivastava, N., Bhagavath, S., Karagadde, S.: Effect of in situ Al3Zr particles on controlling the pore morphology of Al6061 alloy foams. Mater. Today Commun. 26, 101853 (2021). https://doi.org/10.1016/j.mtcomm.2020.101853

[17] An, X., Liu, Y., Ye, J., Li, X.: Fabrication of in-situ TiC–TiB2 reinforced Al foam with enhanced properties, (2020)

[18] Yang, X., Yang, K., Wang, J., Shi, C., He, C., Li, J., Zhao, N.: Compressive Response and Energy Absorption Characteristics of In Situ Grown CNT-Reinforced Al Composite Foams. Adv. Eng. Mater. 19, 294–302 (2017). https://doi.org/10.1002/adem.201700431

[19] Ma, S., Zhuang, X., Wang, X.: Particle distribution-dependent micromechanical simulation on mechanical properties and damage behaviors of particle reinforced metal matrix composites. J. Mater. Sci. 56, 6780–6798 (2021). https://doi.org/10.1007/s10853-020-05684-2

[20] Pandee, P., Sankanit, P., Uthaisangsuk, V.: Structure-mechanical property relationships of in-situ A356/Al3Zr composites. Mater. Sci. Eng. A. 866, (2023). https://doi.org/10.1016/j.msea.2023.144673

[21] Dao, M., Chollacoop, N., Van Vliet, K.J., Venkatesh, T.A., Suresh, S.: COMPUTATIONAL MODELING OF THE FORWARD AND REVERSE PROBLEMS IN INSTRUMENTED SHARP INDENTATION. (2001)

[22] Okereke, M.I., Akpoyomare, A.I.: A virtual framework for prediction of full-field elastic response of unidirectional composites. Comput. Mater. Sci. 70, 82–99 (2013). https://doi.org/10.1016/j.commatsci.2012.12.036

[23] Akpoyomare, A.I., Okereke, M.I., Bingley, M.S.: Virtual testing of composites: Imposing periodic boundary conditions on general finite element meshes. Compos. Struct. 160, 983–994 (2017). https://doi.org/10.1016/j.compstruct.2016.10.114

[24] Zhou, J., Gokhale, A.M., Gurumurthy, A., Bhat, S.P.: Realistic microstructural RVE-based simulations of stress-strain behavior of a dual-phase steel having high martensite volume fraction. Mater. Sci. Eng. A. 630, 107–115 (2015). https://doi.org/10.1016/j.msea.2015.02.017

[25] Yang, X., Hu, Q., Du, J., Song, H., Zou, T., Sha, J., He, C., Zhao, N.: Compression fatigue properties of open-cell aluminum foams fabricated by space-holder method. Int. J. Fatigue. 121, 272–280 (2019). https://doi.org/10.1016/j.ijfatigue.2018.11.008

[26] Bensalem, I., Benhizia, A.: Novel design of irregular closed-cell foams structures based on spherical particle inflation and evaluation of its compressive performance. Thin-Walled Struct. 181, (2022). https://doi.org/10.1016/j.tws.2022.109991

[27] Abstract of : ISO 13314 : 2011 Mechanical testing of metals — Ductility testing — Compression test for porous and cellular metals Foreword 1 Scope 2 Normative references 3 Terms and definitions. 1–3